D19-46
7P.

3.1.5 EVIDENCE OF ATMOSPHERIC GRAVITY WAVE PERTURBATIONS OF THE BRUNT-VAISALA FREQUENCY IN THE ATMOSPHERE

R. E. Good, R. W. Beland, J. H. Brown, and E. M. Dewan

Air Force Geophysics Laboratory
Hanscom AFB
Bedford, MA 01731

A series of high altitude, medium resolution, measurements of temperature, pressure and turbulence have been performed by the Air Force Geophysics Laboratory. These measurements were conducted using the VIZ Manufacturing Co. microsondes with attached AFGL micro-thermal probes measuring the temperature structure coefficient C_T (BROWN et al., 1982). A typical atmospheric temperature measurement is shown in Figure 1. Several small temperature inversions are evident in the troposphere. The stratosphere is marked with numerous fluctuations in the temperature profile. Microsondes provide temperature and pressure measurements every 4 seconds up to a maximum altitude of 30 km (MSL). Since the average ascent rate is 5 m/s, the altitude interval between the measurement reports is 20 m. The potential temperature is calculated from the temperature and pressure from the definition (COLE, 1970):

$$\theta = T \left| \frac{1000}{P} \right|^{R/C_p}$$

where T is the temperature in Kelvins with a resolution of 0.1 K and P is pressure in millibars, R is the ideal gas constant and C_p is the specific heat of air at constant pressure. This equation defines the potential temperature for adiabatic displacements relative to the 1000 mb level. The nominal ratio of R to C_p has the value 0.286.

The Brunt-Vaisala frequency squared, N^2, is defined by

$$N^2 = \frac{g}{\theta} \frac{d\theta}{dz}$$

A problem of computing the Brunt-Vaisala frequency from the microsonde data is thus one of numerical differentiation. Some smoothing of the data is essential due to the tendency that numerical differentiation has in amplifying high frequencies, and hence, noise. Such filtering reduces the spatial resolution of N^2. However, the competing interests of maximizing resolution while minimizing noise must be balanced. The filtering adopted here has two steps. The first filter is a simple 5-point moving average filter. Smoothed potential temperature ($\bar{\theta}$) is computed by:

$$\bar{\theta}_j = \sum_{k=-2}^{+2} \theta_{j-k}/S$$

The transfer function of this filter is:

$$A(k) = \frac{1}{5} \frac{\sin(5k/2)}{\sin(k/2)}$$

The transfer function is displayed in Figure 2. This is a simple low-pass filtering scheme that reduces the vertical resolution of the data from 20 m to approximately 50 m (one half the wavelength of the first null in the transfer function). The sidelobes of this filter are significant. After a differencing, these lobes are much larger than the main peak due to the fact that differentiation corresponds to multiplication by k in the Fourier domain. To overcome this sidelobe problem, a second-stage filter is employed. This stage is a 13-point least squares parabola, i.e., the previous and succeeding 6 points are used to smooth the center of the data. The transfer function of this parabolic filter is also shown in Figure 2. This too is a form of a low-pass filter which reduces the resolution of the data to approximately 75 m.

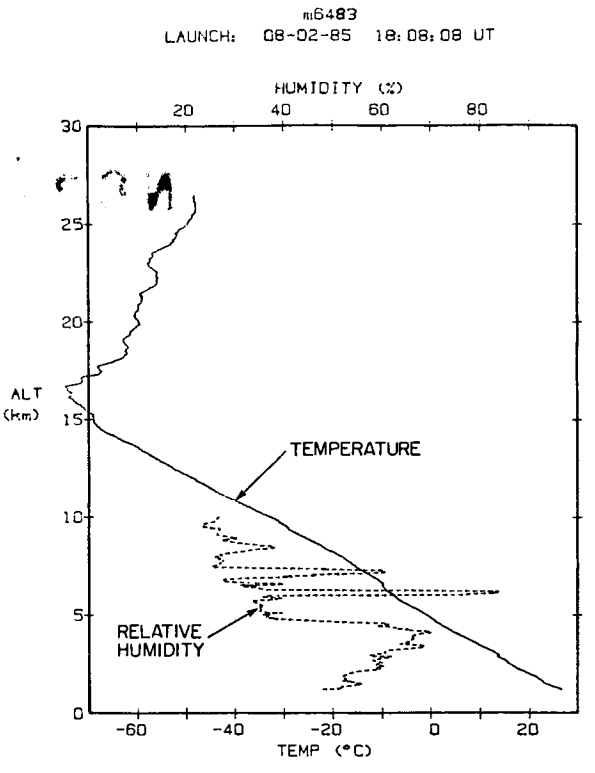

Figure 1. Microsonde temperature profile, Flight M6483 on August 3, 1985 at noon local time, using a standard rod thermistor.

The useful feature of this two-stage filter is that the parabolic sidelobes tend to cancel the moving average sidelobes. This cancellation holds only for certain combinations of orders of the parabola and moving average. The net two-stage transfer function is shown in Figure 2. The potential temperature is smoothed in this two-stage fashion. A further useful feature of the second-stage parabolic filter is that the filter form is a polynomial which is easily differentiated. The transfer function of this differentiating filter is shown in Figure 2. The spatial resolution of the differentiator is approximately 100 m. This is the method of determining the vertical potential temperature gradient; the least squares parabola is differentiated after the first smoothing with the moving average. The Brunt-Vaisala frequency is then calculated using this derivative and the two-stage smoothed potential temperature. The actual derivative can be considered as having occurring over dz of about 300 m. Shorter wavelengths are attenuated.

A typical Brunt-Vaisala frequency squared profile is shown in Figure 3. Depending upon the atmospheric boundary layer conditions, there may exist static instability conditions as indicated when the Brunt-Vaisala frequency is negative. Above 5 km altitude, the Brunt-Vaisala frequency averages to around 0.01 sec^{-1}, while in the stratosphere, the frequency was about 0.025 sec^{-1}. The wave-like structure apparent throughout the atmosphere exhibits different

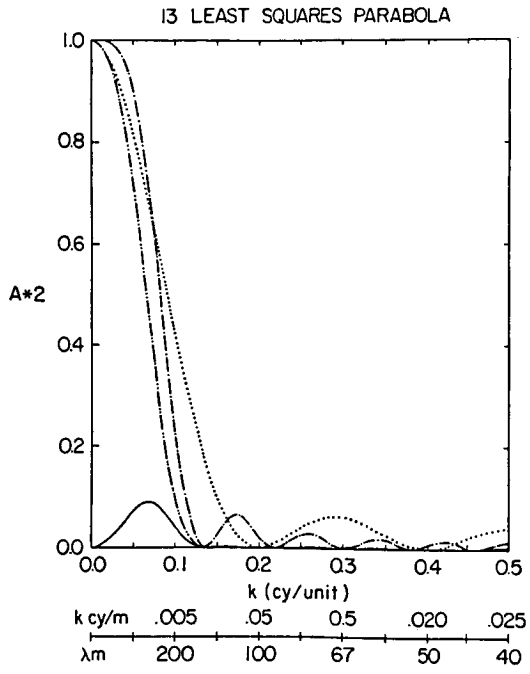

Figure 2. Numerical filters used in smoothing and differentiation. Data initially smoothed with 5-point moving average (– – –), then fitted with a 13-point parabola (–·–·–·–·–·–). These are combined as shown by the (–··–··–··–··–) curve. Differentiation of the combined the 5-pt and 13-pt parabola (————) yields the Brunt-Vaisala frequency.

characteristic scales in the troposphere and the stratosphere. An examination of Figure 3 indicates a visual periodicity of 1 to 3 km in the stratosphere and less than 1 km in the troposphere. The Brunt-Vaisala frequency transition between the troposphere and the stratosphere generally occurs over a 1- to 4-km altitude region.

A power density spectra was obtained of the Brunt-Vaisala frequency squared to examine possible periodicities in the wave-like structures. The procedure applied was to use the Blackman-Tukey approach of (1) de-trending the data by removing a mean, (2) obtaining the truncated autocorrelation, (3) Hamming the autocorrelation and then (4) computing the power spectral density (PSD) of N^2, § $(rad/s)^4/(cy/m)$, as a function of wave number, k (cy/m). Note that no pre-whitening and subsequent post-darkening is applied. The reason for not doing this is that we are interested only in the low frequencies. Furthermore, the data have been extensively smoothed which avoids aliasing errors in the PSD. We have also used a minimum entropy method linear predictor with 20 and 40 coefficients. The 20 coefficients are used to obtain smooth PSD plots to examine the envelope. The 40 coefficients are used to identify specific wave number contributions.

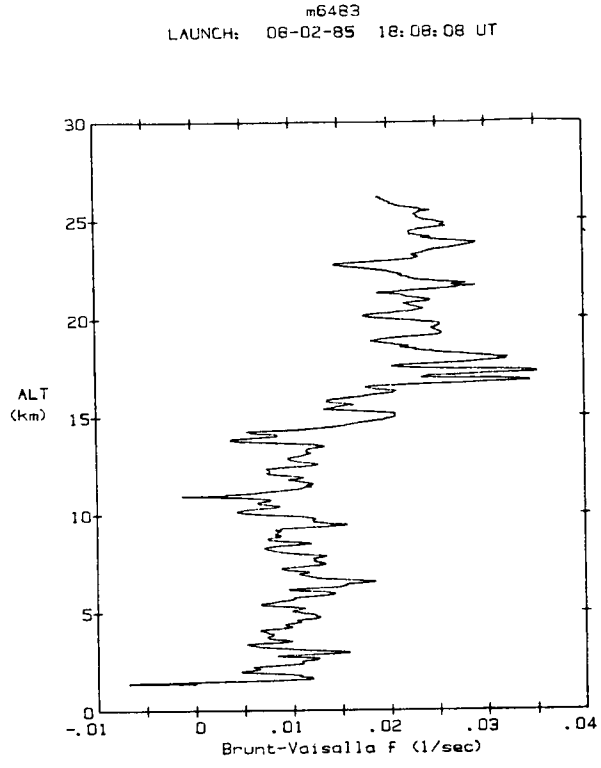

Figure 3. Calculated Brunt-Vaisala frequency, Flight M6483.

Figures 4a and 4b represent the PSD of the vertical spatial profile of the squared Brunt-Vaisala frequency for the microsonde flights shown in Figure 3. The stratospheric region is defined as being between 17 km to 27 km and the troposphere is defined as between 2.5 and 14 km. The spectral envelope is one of constant PSD to the maximum wave number, k*. The PSD decreases as the wave number increases from k* to the filter cutoff, $k_f = 1/200\ m^{-1}$. A detailed look at the spectrum shows 2-4 identifiable peaks. This is interpreted as indicating a narrow selection of gravity waves in the stratosphere and not a continuous array of wavelengths. This can be visualized in Figure 5 which is an expanded graph of the Brunt-Vaisala data.

Finally, we have combined the spectra from four soundings (M5309, M6472, M6474, and M6483) and obtain an average PSD for the troposphere and the stratosphere shown in Figure 5. Shown here is the fact that the spectra can be considered to have a -1 slope between 4 km and the 300-m wavelength of the filter. The stratosphere amplitude is about an order of magnitude larger than the troposphere amplitude.

FRITTS (1984) and WEINSTOCK (1984) have indicated that gravity-wave saturation should occur simultaneously with the existence of convective instability regardless of whether or not the saturation mechanism is due to Kelvin-Helmholtz instability, nonlinear wave interactions, or direct

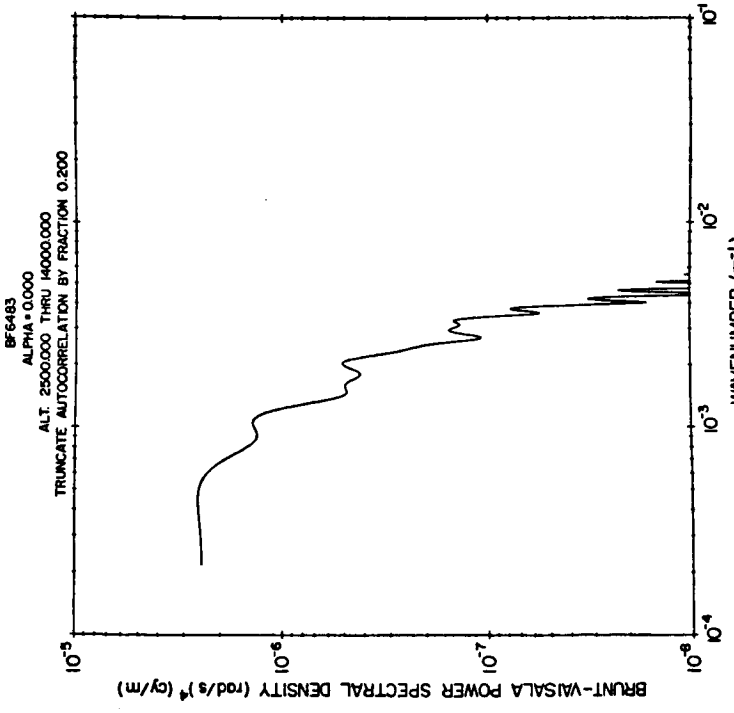

Figure 4a. Power spectral density of tropospheric Brunt-Vaisala frequency squared (Flight M6483) for the altitude region between 2.5 and 14 km.

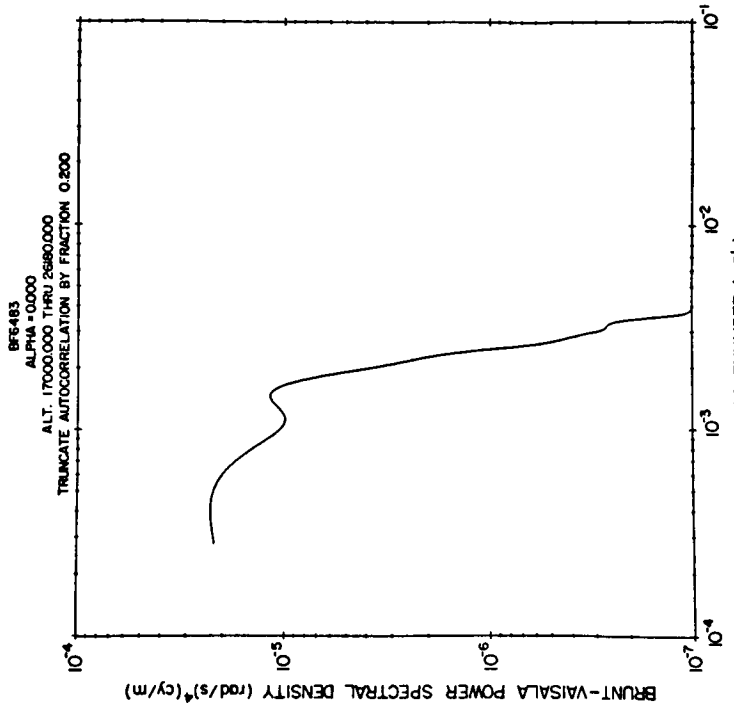

Figure 4b. Power spectral density of stratospheric Brunt-Vaisala frequency squared (Flight M6483) for the altitude region between 17 and 27 km.

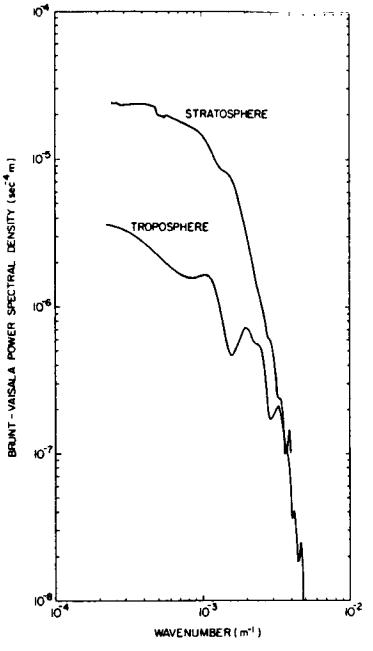

Figure 5. Comparison of the power spectral density of the stratosphere and troposphere. Each curve represents the linear average of four PSDs obtained from flights M6483, M5309, M6472, M7474 from July 31 to August 3, 1985.

convective instability. The fact that we do not see convective instabilities above the boundary layer (as indicated by negative Brunt-Vaisala frequencies), may be due to the following reasons. First, the instability produces turbulence at scales less than 100 m and have been filtered out of this presentation. This is consistent with the detailed turbulent layer measurements of BARAT and BERTIN (1984). Second, the microsonde thermistor rod has a long time constant ($t \sim 15$ seconds at 25 km, 7.8 sec at 15 km) and is unable to accurately respond to the presence of 20- to 40- m thick regions exhibiting adiabatic lapse rates. We are presently conducting experiments using both bead and rod thermistors. The hope is that the bead thermistor, while having errors in absolute temperature, will indicate the small-scale regions of adiabatic lapse rate owing to their fast time constant ($t \sim .3$ second).

The source of the wave-like structure is assumed to be gravity waves. DEWAN and GOOD (1985) have suggested that gravity waves grow in amplitude during passage up through the atmosphere. However, a maximum growth is reached when the saturation conditions occur. The saturation instability leads to the production of turbulence. The spectra of vertical profile of horizontal winds observed in the stratosphere has been shown by DEWAN and GOOD (1985) and SMITH et al. (1985) to exhibit a -3 slope for all wavelengths greater than the dominate wavelength, k*. The question that needs to be answered is, What is the mechanism for producing the wave-like structure in the Brunt-Vaisala frequency? An explanation is that the gravity waves themselves alter the Brunt-Vaisala frequency in the atmosphere. HODGES (1967) estimates the density and temperature perturbations of a gravity wave. It can be shown that the squared Brunt-Vaisala power density spectrum under gravity-wave saturation hypothesis will have a slope of -1.

Thus, the temperature changes that can be produced by a gravity wave are small unless nonlinear effects are occurring. Such nonlinear interactions can occur and themselves limit the growth of gravity waves. FRITTS (1984) has shown that these nonlinear interactions can produce a gravity-wave spectrum similar to the saturation theory.

CONCLUSIONS

Spectral analysis of atmospheric Brunt-Vaisala frequencies reveal spectra similar to the velocity spectra of DEWAN et al. (1984), DANIELS (1982), and ENDLICH and SINGLETON (1969). The Brunt-Vaisala spectra indicate existence of separate, distinguishable wave modes.

REFERENCES

Barat, J., and F. Bertin (1984), Simultaneous measurements of temperature and velocity fluctuations within clear air turbulence layers: Analysis of the estimate of dissipation rate by remote sensing techniques, J. Atmos. Sci., 41, 1613-1619.

Brown, J. H., R. E. Good, P. M. Bench, and G. Faucher (1982), Sonde experiments for comparative measurements of optical turbulence, AFGL-TR-82-0079.

Cole, F. (1970), Introduction to Meteorology, John Wiley & Sons, N.Y.

Daniels, G. (1982), Terrestrial environment (climatic) criteria guidelines for use in aerospace vehicle development, 1982 Revision NASA Tech. Memo, NASA TM-82473.

Dewan, E. M., N. Grossbard, A. F. Quesada, and R. E. Good (1984), Spectral analysis of 10 m resolution scaler velocity profiles in the stratosphere, Geophys. Res. Lett., 11, 80-83 and 624.

Dewan, E. M., and R. E. Good (1985), Saturation and the universal spectrum for vertical profiles of horizontal scaler winds in the atmosphere, submitted to J. Geophys. Res..

Endlich, R. M., and R. C. Singleton (1969), Spectral analysis of detailed vertical wind speed profiles, J. Atmos. Sci., 26.

Fritts, D. C. (1984), Gravity wave saturation in the middle atmosphere: A review of theory and observations, Rev. Geophys. Space Phys., 22, 275-308.

Hodges, R. R., Jr. (1967), Generation of turbulence in the upper atmosphere by internal gravity waves, J. Geophys. Res., 72, 3455-3458.

Smith, S., D. C. Fritts, and T. E. VanZandt (1985), Evidence of a saturation spectrum of atmospheric gravity waves, submitted to Geophys. Res. Lett..

Weinstock, J. (1984), Gravity wave saturation and eddy diffusion in the middle atmosphere, J. Atmos. Terr. Phys., 46, 1069-1082.